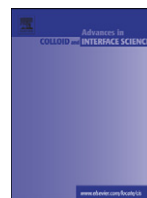




ELSEVIER

Contents lists available at ScienceDirect

## Advances in Colloid and Interface Science

journal homepage: [www.elsevier.com/locate/cis](http://www.elsevier.com/locate/cis)

## On a tweezer for droplets

John W.M. Bush<sup>a</sup>, François Peaudecerf<sup>a</sup>, Manu Prakash<sup>b</sup>, David Quéré<sup>c,\*</sup><sup>a</sup> Department of Mathematics, MIT, Cambridge, MA 02139, USA<sup>b</sup> Society of Fellows, Harvard University, Cambridge, MA 02138, USA<sup>c</sup> Physique et Mécanique des Milieux Hétérogènes, ESPCI, 75005 Paris, France

## ARTICLE INFO

Available online xxxx

## Keywords:

Contact angle hysteresis

Self-propulsion

Capillary ratchet

## ABSTRACT

We describe the physics behind a peculiar feeding mechanism of a certain class of shorebirds, in which they transport their prey in droplets from their beak tips mouthwards. The subtle interplay between the drop and the beak's tweezer motion allows the birds to defy gravity through driving the drop upwards. This mechanism provides a novel example of dynamic boundary-driven drop motion, and suggests how to design tweezers for drops, able to trap and to move small amounts of liquid.

© 2010 Published by Elsevier B.V.

## Contents

1. The feeding technique of phalarope . . . . .	0
2. Self-propulsion . . . . .	0
3. Mandibular propulsion . . . . .	0
4. Conclusion . . . . .	0
Acknowledgements . . . . .	0
References . . . . .	0

## 1. The feeding technique of phalarope

Phalaropes are small birds that inhabit the American and Russian coastlines of the Arctic Ocean [1]. Discovered by George Edwards in the eighteenth century, they were later described and named by Brisson «because their feet resembled those of a coot» – *phalaris* in Greek, according to Buffon [2]. They were first known for their task sharing: the larger females migrate southwards (toward the Sea of Oman) soon after the egg-laying season, while the males hatch the eggs before caring for the young. But their peculiar feeding technique, first discovered by Rubega et al. in the nineties, is even more curious [3,4]. The phalarope bill is short, 1–3 cm in length [5]. Since it does not dive, it is obliged to draw its sustenance from the immediate vicinity of the surface. The solution to this problem is, literally, revolutionary: the phalarope swims close to the shore in tight circles, at a speed of order 50 cm/s, generating an upward flow leading to transport of prey, crustaceans and plankton, from the bottom towards the surface [6]. The bird then serves itself by rapidly striking its beak (approximately twice per second) [2,5,7,8]. With each peck, it

captures a prey-laden water droplet (Fig. 1). Since the bill generally points downwards, the drop moves upwards to the throat where the phalarope pins the contained prey (typically one per drop) with its tongue, then swallows it. The question naturally arises as to how the liquid moves against gravity, and what are the characteristics of this tweezer for droplets.

We recently published a first paper devoted to the description of this device [9]. The aim here is to make clear a few new points. After recalling the mechanism of self-propulsion, we model the dynamics of the drop when it wets the tweezer – a point that was not discussed properly in [9]. Then we focus on the case of partial wetting, generally relevant when the liquid is water. We quantify how a drop is propelled by a tweezer action that exploits the drop asymmetry, by a tweezer action resulting from the conjunction of pinning and geometry. We specify in particular the typical displacement of the drop per cycle, allowing us to define the efficiency of the tweezer, and stress the effects of gravity, when it opposes the motion.

## 2. Self-propulsion

Before we take a closer look at the origin of the movement, we note that the drop must form a bridge between the upper and the lower

\* Corresponding author.

E-mail address: [david.quere@espci.fr](mailto:david.quere@espci.fr) (D. Quéré).

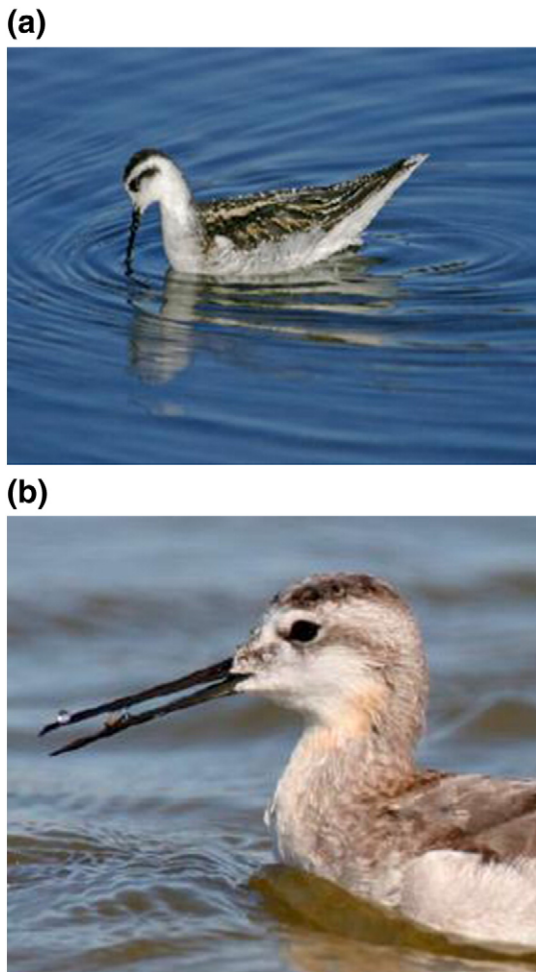


**Fig. 1.** Photographs of two phalaropes in action. (a) Red-neck phalarope extracts a prey-bearing droplet from the free surface. (b) Wilson phalarope drives the droplet mouthward, not by applying suction, but by opening and closing its beak in a tweezer motion. (Photo Credit: Robert Lewis.)

bills. This puts an upper bound on the opening angle because a drop can only join two planes if the distance between them is no more than the width of the drop [10]. Otherwise, it breaks into two separate drops, one on either plane. The drop size is typically the capillary length  $\ell_c = (\gamma/\rho g)^{1/2}$ , that is, a few millimeters. The gap between the tips of a bill of length  $L_b$  opened by an angle  $\alpha$  scales as  $\alpha L_b$ , so that the stability condition can be roughly written  $\alpha < \alpha_c \sim \ell_c/L_b$ , which yields a critical angle of only a few degrees. If it opens its bill too wide, a clumsy phalarope may lose its meal, just like the greedy crow of the fable.

The manner in which water drops can be propelled along a bird beak is qualitatively different according to the wettability of the beak, which can be modified by chemical contamination. For the case of pure wetting, a molecular film of fluid spreads to wet the entire beak, thus eliminating contact lines and the complications arising therefrom. We proceed in this section by describing the dynamics in this case, but note that it is more of academic interest than directly relevant to the shorebirds. Water partially wets keratin, the material comprising bird beaks; consequently, a water drop inside the beak of the phalarope is bound by contact lines, where the drop surface meets the solid [2]. As we shall see in Section 3, the means of propulsion in this case is entirely different.

Our experimental study enabled us to characterize the horizontal motion of oil wetting drops along artificial beaks with shapes similar to those of the phalarope [9]. A wetting drop placed at the end of the artificial bill is sucked mouthward, as shown in Fig. 2 where we

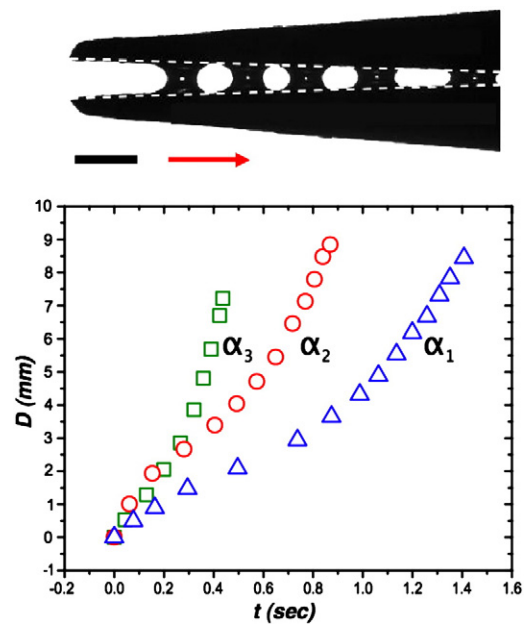


**Fig. 2.** The time evolution of the position  $D$  of a drop of silicon oil (viscosity  $\eta=20$  mPa s, surface tension  $\gamma=20$  mN/m) in a horizontal artificial bill. The arrow indicates the direction of motion, and the scale bar, 2 mm. The graph shows that the drop accelerates as it progresses towards the confined part of the bill. The angles  $\alpha_1$ ,  $\alpha_2$  and  $\alpha_3$  are equal to  $1.9^\circ$ ,  $2.8^\circ$  and  $4.2^\circ$ , respectively. At long time, the larger the angle, the faster the motion: the corresponding terminal velocities are found to be  $1.05 \pm 0.20$ ,  $1.60 \pm 0.10$  and  $2.60 \pm 0.30$  cm/s [9].

display the distance  $D$  traveled by the drop as a function of time for three different angles  $\alpha$ . The geometry in the direction perpendicular to the axis of the beak is simplified by the small size (2 mm) of its width  $W$ : hence, the drop (of length  $L$  always larger than  $W$ ) pins along the lateral sharp edges, and the discussion reduces to the description of the menisci directly visible in Fig. 2. The gap across the bill decreases toward the mouth, so that a drop there assumes a fore-aft asymmetric shape. The curvatures of the menisci bounding the drop differ, generating a differential Laplace pressure along the length of the drop that propels the drop towards the narrower end, hence mouthward [9,11]. A reversed wettability would change the sign of the Laplace pressure, and thus the direction of the motion.

Using the definitions of Fig. 3, the Laplace depressions at the leading and trailing edges of a wetting drop ( $\theta_1 = \theta_2 = 0$ ) scale in absolute value as  $\gamma/\alpha x$  and  $\gamma/\alpha(x+L)$ , where  $\gamma$  is the liquid surface tension. Therefore, the pressure difference between leading and trailing edges is  $\gamma L/\alpha x^2$ , assuming that drops are small relative to the distance to the mouth ( $L \ll x$ ). Integrating over the menisci surface areas  $\alpha x$  (written per unit width of the beak) yields a Laplace force  $\gamma L/x$  that draws the drop mouthwards, to the right in Figs. 2 and 3.

As the drop moves, this force is balanced by a viscous friction. Here there are two possibilities, as always when dealing with moving drops: the force is dominated by either contact line friction, or a bulk (Poiseuille-type) friction on the surface  $L$  (per unit width) of the bill. Denoting  $\eta$  as the viscosity of the liquid, we can evaluate and compare these forces, written per unit width of the beak.

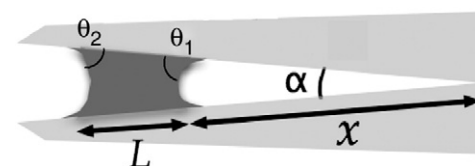


**Fig. 3.** Drop of length  $L$  in a bill opened by an angle  $\alpha$ , at a distance  $x$  from the mouth.

For the line friction, we adopt a simple physical picture, though recognize that many subtle features may complicate the discussion. For a wetting liquid, the line friction along an advancing front is due to the local divergence of the velocity gradient close to the moving front. It is expected to scale as  $\eta V/\theta$ , where  $\theta$  denotes the dynamic contact angle at the leading edge [12,13]. This angle should obey Tanner's law,  $\theta \sim (\eta V/\gamma)^{1/3}$ , where we again neglect the numerical coefficients. There thus arises a friction force  $F_1 \sim \gamma (\eta V/\gamma)^{2/3}$ . The Poiseuille resistance is easier to evaluate: since the gap in the bill is  $\alpha x$ , this viscous stress scales as  $\eta V/\alpha x$ , which, once integrated along the drop length yields:  $F_2 \sim \eta LV/\alpha x$ . When the velocity is small, and the drop far from the mouth (i.e.  $x$  large and  $L$  small), we expect the line friction to be dominant ( $F_1 \gg F_2$ ). We find, after balancing it with the capillary propulsive force in the  $L \ll x$  limit:

$$V \sim \gamma / \eta (L/x)^{3/2}.$$

This law should describe the first regime (in time) in Fig. 2, when the drop is far from the mouth. Its structure implies that the velocity is not expected to be constant, as observed in Fig. 2: as the liquid advances,  $L$  increases and  $x$  decreases, leading to an acceleration of the drop. In the experiment of Fig. 2, the visco-capillary speed  $\gamma/\eta$  is 1 m/s ( $\gamma = 20$  mN/m and  $\eta = 20$  mPa s) and the geometric factor  $(L/x)^{3/2}$  is between 0.01 and 0.1, for millimetric drops and centimetric bills. This gives initial velocities at the beginning of the motion of approximately 1 cm/s, comparable to the 4 mm/s observed in this regime.

As the drop approaches the mouth, the Poiseuille force becomes dominant compared to the line friction ( $F_2 \gg F_1$ ), and balancing the corresponding formula with the capillary force leads to a remarkably simple formula for the drop speed:

$$V \sim \alpha \gamma / \eta.$$

This speed is constant despite the fact that the length  $L$  of the drop increases with time as it proceeds into the gap. It is the product of the opening angle  $\alpha$ , a small number (of the order of 0.03 to 0.05 rad), by the (large) visco-capillary velocity. The drop velocity  $V$  is thus expected to be on the order of a few centimeters per second, in qualitative agreement with observations reported in Fig. 2 where we find  $V \approx 1$  to 3 cm/s close to the mouth, i.e. at large distances  $D$ . In addition, it is also clear in the same figure that this fast regime is a function of the opening angle  $\alpha$ , and roughly proportional to it: multiplying the angle by a factor 2.2 (from 1.9 to 4.2°), the terminal velocity passes from  $1.05 \pm 0.20$  cm/s to  $2.6 \pm 0.3$  cm/s. Further experiments would be necessary to check quantitatively these different laws.

The crossover between the two regimes of friction occurs when  $\eta LV/\alpha x$  exceeds  $\gamma (\eta V/\gamma)^{2/3}$ , that is, for  $L > \alpha^{2/3} x$ , if we take  $\alpha \gamma/\eta$  as a characteristic drop speed.  $\alpha^{2/3}$  is typically  $1/4$ , so the above inequality is only satisfied for centimetric drops: at the beginning of the movement,  $L$  is a few millimeters, and the dominant friction is indeed the line friction. Subsequently, as the drop enters confined region,  $L$  and  $x$  become comparable, and the speed becomes dictated by the Stokes friction ( $V \sim \alpha \gamma/\eta$ ).  $L$  and  $x$  are related to each other by volume conservation ( $Lx = L_0 x_0$ ), so that the condition for passing from one regime of friction to the other one can be simply expressed in terms of the distance  $x$ , which at the threshold is  $(L_0 x_0)^{1/2}/\alpha^{1/3}$ , i.e. 1 cm typically.

### 3. Mandibular propulsion

It turns out that our phalarope seasons his meal with water, not oil, so the physical picture changes dramatically. Water droplets in both the real and artificial bird beaks are bound by contact lines, which impede their progress. When a small droplet ( $\sim 2$  mm) is placed at the

tip of the horizontal artificial beak, it remains pinned in place at the spot it was inserted, its progress halted by contact angle hysteresis. Specifically, hydrophilic defects hold back the trailing edge of the drop while its leading edge is impeded by their hydrophobic counterparts. This phenomenon is familiar in that it prevents rain droplets from sliding down windows, despite the force of gravity [14]. Indeed, contact angle hysteresis is typically an impediment to drop motion, which makes the phalarope's feeding mechanism all the more remarkable.

The trick of the phalarope is its mandibular movement, alternately squeezing and relaxing the drop [3,4]. The conjunction of a propulsive force with a vibration of large enough amplitude can trigger drop motion [9,15–18]. Such motion is easily recreated in an artificial bill, where we observe that water progresses incrementally in a ratchet-like fashion (Fig. 4). The angle  $\alpha$  is now a function of time, starting from a maximum  $\alpha_M$  and decreasing to a minimum  $\alpha_m$  before increasing back to  $\alpha_M$ , and so on, at a rate  $f$  of 10 cycles per second. This high frequency enables the liquid to move quickly, with an average speed on the order of 10 cm/s. We now discuss why and how this mandibular propulsion occurs, and evaluate its efficiency.

It is first instructive to describe what happens when a drop is placed between two parallel plates that are successively closed and opened in the absence of gravity. As long as the amplitude of the oscillation is sufficiently small, the contact lines remain pinned on the defects of the solid surfaces. Above a threshold in amplitude, the liquid starts moving, alternately spreading and retracting without displacing its center of mass [19]. When the plates approach, the contact angles necessarily increase owing to volume conservation.

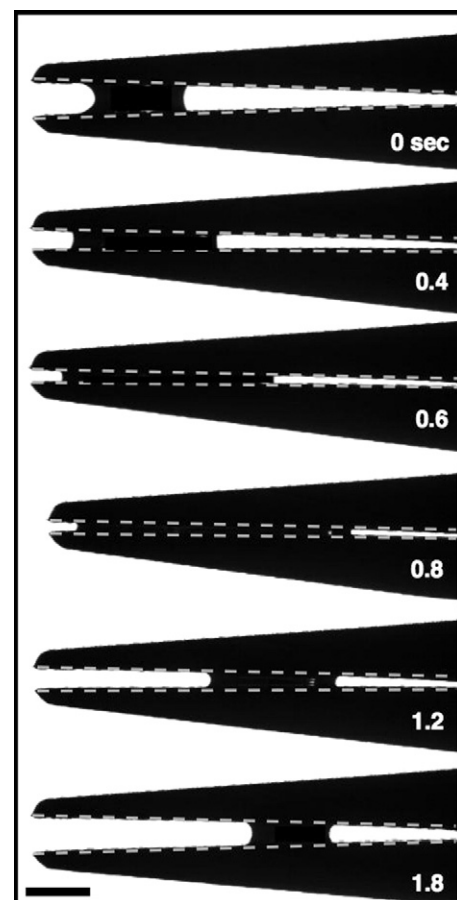


**Fig. 4.** Progression of a water drop in an artificial bill: the drop partially wets the solid and only moves by virtue of the periodic closing and opening of the bill. The average speed is prescribed by the extremal angles and frequency of the mandibular movement. Time is shown on the right, in seconds, and the scale bar on the lower left corner indicates 2 mm.

Depinning takes place when the contact angle exceeds its largest tenable static value, the so-called advancing angle  $\theta_a$ . Similarly, as the plates separate, the contact angles decrease and lines retreat when the angle becomes smaller than the minimum tenable static value, the receding angle  $\theta_r$ . If the plates are tilted to lie in the vertical, the force balance of the drop of volume  $\Omega$  (per unit width  $W$ ) requires that:

$$\rho\Omega g = 2\gamma(\cos\theta_1 - \cos\theta_2),$$

which prescribes the maximum volume  $\Omega_c = 2\ell_c^2(\cos\theta_r - \cos\theta_a)$  that may be supported between the plates, where  $\ell_c$  is again the capillary length. This balance, analogous to that describing the force balance of a raindrop stuck on a window pane [14] yields a valuable relation between  $\theta_1$  and  $\theta_2$ ; specifically, it makes clear that  $\theta_2 > \theta_1$ . Thus, as the gap is closed and the internal drop pressure increased,  $\theta_2$  always reaches  $\theta_a$  before  $\theta_1$ ; consequently, the lower edge of the drop advances first. Conversely, the upper edge is always the first to retreat when the beak is opened. In this vertical planar geometry, opening and closing the gap leads to progressive downward motion: the hydrostatic pressure gradient precludes droplet climbing.

We proceed by considering the beak geometry, in which the plate orientation is characterized by the opening angle  $\alpha$  (Fig. 3). The amplitude of the beak motion during its tweezer action is prescribed by the maximum and minimum opening angles, respectively,  $\alpha_M$  and  $\alpha_m$ . The contact lines move only if the quantity  $\alpha_M - \alpha_m$  is sufficiently large, but this motion may now be accompanied by a net displacement of the drop towards the corner (i.e. the mouth of the phalarope) (Fig. 4). We consider in turn the beak geometry in the absence and presence of gravity, in order to describe drop motion on horizontal and vertical beaks.

In the absence of gravity, the pressure inside the static drop is uniform; therefore, the radii of curvature on the drop edges are equal, a geometric condition that requires:

$$\cos(\theta_2 + \alpha/2) = (1 + L/x) \cos(\theta_1 - \alpha/2),$$

This yields a relationship between the contact angles  $\theta_1$  and  $\theta_2$ . In the limit  $L \ll x$ , it assumes the simple form  $\theta_1 = \theta_2 + \alpha$ : geometry requires that  $\theta_1$  always exceed  $\theta_2$ . When the bill is closed, the advancing angle  $\theta_a$  will first be achieved by  $\theta_1$ . The front of the drop will thus advance, while its trailing edge remains pinned (Fig. 5). If the bird closes its bill too far, the contact angle  $\theta_2$  will also reach  $\theta_a$  so that the trailing edge also moves, but in the opposite direction. When the bill opens, the motions are reversed: the trailing edge moves first, receding mouthward when  $\theta_2$  reaches  $\theta_r$ . In the opening phase, the leading edge will also recede if  $\theta_1$  reaches  $\theta_r$ . Hence, there is an incremental motion of the drop for each half-cycle, provided the amplitude of the mandibular motion is neither too small (in which case both contact lines remain pinned) nor too large (in which case both lines move). Note that the conjunction of asymmetry and vibration was shown to lead to a movement in a different system, namely partially wetting drops on inclines, which, when vibrated, can lead to uphill motions [20].

Besides providing an explanation for the drop motion, our discussion makes clear that the propulsion can be optimized. If the phalarope finely tunes the extrema angles  $\alpha_M$  and  $\alpha_m$ , it can advance only the leading edge during its closing phase (leaving the trailing edge pinned), and the trailing edge during its opening phase (leaving the leading edge pinned). This progression is depicted in the first three steps of Fig. 5, and results in a purely mouthward drop motion. It was shown on artificial, horizontal bills that there is indeed a narrow window of opening and closing angles that minimizes the number of cycles required for moving a drop along a prescribed length [9].

Phalaropes typically feed themselves with their beaks pointing down towards the water, and so necessarily draw the drops upwards. Consequently, the mouthward motion of drops induced by their

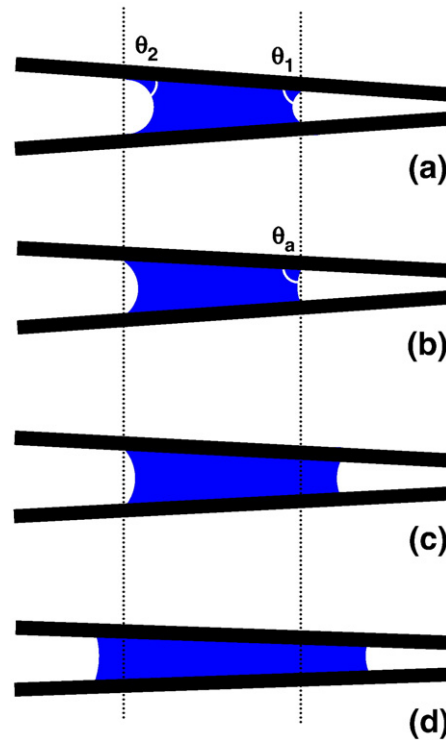


Fig. 5. (a) In a situation of partial wetting, drops may be pinned in the bill, owing to the anchoring of the contact lines on the substrate defects. (b) When the phalarope closes its bill, both angles increase, but the front angle  $\theta_1$  is the first to reach the advancing angle  $\theta_a$  above which motion takes place; thus, only the leading edge starts progressing (c). (d) If the phalarope further closes its bill,  $\theta_2$  can also reach  $\theta_a$ , which induces a motion of the trailing edge in the opposite direction.

mandibular cycles will be opposed by gravity. We proceed by demonstrating how vertical motion may be attained and gravity overcome in the bird beak geometry. We assume that gravity is important in establishing a vertical hydrostatic pressure along the length of the drop, but that the upper and lower drop surfaces are still circular arcs to leading order, an assumption valid provided the local gap width  $\alpha$  is smaller than  $\ell_c$ . For a vertical beak, the curvature force must now support the weight of the drop:

$$\cos(\theta_2 + \alpha/2) = (1 + L/x) \cos(\theta_1 - \alpha/2) - (x + L)L \tan(\alpha/2) / \ell_c^2.$$

This equation defines the maximum drop volume  $\Omega_M$  (per unit width  $W$ ) that can be sustained within the bill. In the limit of  $L \ll x$ , this assumes the simple form:

$$\Omega_M = 2\ell_c^2(\cos(\theta_r - \alpha/2) - \cos(\theta_a + \alpha/2)).$$

Moreover, it yields a relation between  $\theta_1$  and  $\theta_2$  from which we see that  $\theta_1$  may be either greater or less than  $\theta_2$ , depending on the Bond number  $Bo = \Omega/\ell_c^2$ . In the small Bond number limit, this relation may be expressed as:

$$\theta_1 = \theta_2 + \alpha - \Omega / (2\ell_c^2 \sin((\theta_1 + \theta_2)/2))$$

Accordingly, the mandibular motion will cause the drop either to rise or fall depending on the magnitude of the Bond number, specifically on the sign of the quantity  $\alpha - Bo/(2\sin((\theta_1 + \theta_2)/2))$ . We see in particular that a critical Bond number  $Bo_c$  of the order  $\alpha$  must not be exceeded if the drop is to be drawn mouthward along vertical bills. Combining this dynamic condition,  $Bo < \alpha$ , with that required to avoid drop cleavage,  $\alpha_c < \ell_c/L_b$ , indicates that the vertical ratcheting mechanism can only operate if the drop volume  $\Omega$  per unit

width is smaller than  $\ell_c^3/L_b$ , a quantity of the order of  $1\text{ mm}^2$  (corresponding to  $2\text{ mm}^3$  for a width of  $2\text{ mm}$ ).

In the optimized situation, we can evaluate the drop progression generated by a mandibular cycle and so deduce the delivery time of the phalarope's meal. For the sake of simplicity, we again consider compact drops ( $L \ll x$ ). For small bill angles, we also assume  $\alpha x \ll L$ . This allows us to neglect the contribution of the menisci to the drop volume  $\Omega \approx 1/2\alpha(x_2^2 - x_1^2)$ , where  $\Omega \approx \alpha Lx$  is written per unit width of the bill, and  $x_1$  and  $x_2$  denote the positions of the leading and trailing drop edges, respectively. In this limit, volume conservation requires that:  $x_2 = (x_1^2 + 2\Omega/\alpha)^{1/2}$ . Since the position  $x_1$  of the leading edge remains fixed in the optimized cycle, we deduce that the progression  $\Delta x_2$  of the trailing edge resulting from a mandibular opening  $\Delta\alpha$  can be written:  $\Delta x_2 \approx \Omega\Delta\alpha/(\alpha^2 x)$ . A similar expression is obtained for the advancement  $\Delta x_1$  of the leading edge when the bill is closed by the same angle  $\Delta\alpha$ . We thus deduce the total progression  $\Delta x$  of the drop in one cycle:

$$\Delta x \approx 2\Omega\Delta\alpha / (\alpha^2 x) \approx 2L\Delta\alpha / \alpha.$$

In the limit considered here,  $L$  is of the order of the capillary length ( $3\text{ mm}$ ), which, for  $\Delta\alpha/\alpha = 1/2$ , yields a progression  $\Delta x$  of  $3\text{ mm}$ . In our model, the bird needs 3 to 9 mandibular cycles to drive the drop along the bill, whose length  $L_b$  is approximately 1 to 3 cm, consistent with data on phalaropes [8]. The corresponding velocity  $V$  is  $2Lf\Delta\alpha/\alpha$ , where  $f$  is the number of cycles per second. The mandibular frequency  $f$  is typically 10 Hz, which means that less than 1 s is needed for the drop transport, a time comparable to the period between two bird's pecks. The progression is not constant: since  $L$  increases as the drop approaches the mouth, so do  $\Delta x$  and  $V$ .

In the opposite limit of flattened drops, for which  $L \gg x$ , the drop volume can be written  $\Omega \approx \alpha L^2/2$ . Conservation of volume implies that the change in length  $\Delta L$  of the drop arising from an angle variation  $\Delta\alpha$  satisfies the relation:  $2\Delta L/L \approx \Delta\alpha/\alpha$ . This yields a drop progression per cycle  $\Delta x \approx 2\Delta L$  that follows the same scaling law as previously:  $\Delta x \approx L\Delta\alpha/\alpha$ . Since  $L$  is centimetric in this flattened-drop limit, very few cycles (of order 1 to 3, typically, depending on  $\Delta\alpha/\alpha$ ) are necessary to drive the drop to the mouth, consistent with experimental and field observations [2,9]. The corresponding (average) velocity  $Lf\Delta\alpha/\alpha$  is high, typically 10 cm/s or more, depending on the chosen frequency  $f$ .

#### 4. Conclusion

We have considered how drop propulsion occurs in wedge-like geometries. The first case applies for situations in which the fluid completely wets the substrate. Here, differential curvatures associated with the beak geometry result in a pressure gradient capable of driving the drop to the tip of the wedge. We have demonstrated that such motion is generally opposed by resistance associated with viscous dissipation in the bulk of the drop and line friction near its advancing edges. Balancing the propulsive force  $\gamma L/x$  with the weight of the drop suggests that such capillary propulsion would drive drops upwards in a vertical beak provided  $Bo = \rho g \Omega / \gamma < L/x$ , which represents a strong constraint (often impossible to satisfy) in the limit  $L \ll x$  where this condition can be also written  $\alpha x^2 < \ell_c^2$ .

In the case of partial wetting, we emphasized the necessity of imposing tweezing effect to overcome pinning of the contact line. While one would expect contact angle hysteresis to resist drop propulsion, it couples in this case to the wedge-like geometry to drive the drop towards the corner, mouthwards in the case of shorebirds, in a stepwise ratcheting fashion. Ideally, the minimum and maximum opening angles are such that only one contact line moves per opening or closing event, in which case the efficiency of the motion can be deduced from volume conservation. On a vertical beak, the drop's ascent is resisted by gravity: only drops such that  $Bo < \ell_c/L_b$  should be capable of climbing. This implies that the quantity of water extracted by the phalaropes must be carefully selected, which remains to be proven. We also note that this constraint is comparable to that which applies to curvature-driven drop motion on a wetting beak. However, the ratchet mechanism has the distinct advantage of setting the drop speed by the frequency of the mandibular cycle, and so may be increased arbitrarily.

Our study also highlights the extreme sensitivity of the phalarope to pollution. In the presence of oil or detergents, water can wet the bill. Then, hysteresis is eliminated, gravity makes the drop flow downwards, and the phalarope's meal can no longer be raised to its mouth. Despite being large relative to the capillary length, the phalarope has a feeding mechanism that relies critically on the surface tension of water, making it particularly fragile in the presence of contaminants [3,21]. More generally, the physical mechanism elucidated herein provides all the ingredients of a fluid tweezer: it retains drops, and allows them to be manipulated and driven in a given direction.

#### Acknowledgements

The authors thank Jean-Pierre Hulin and Charles-Henri de Novion for excellent suggestions, and for allowing them to use material published in French in *Reflets de la Physique* on the same theme.

#### References

- [1] M.A. Rubega, D. Schamel, D. M. Tracy, Red-necked phalarope (*Phalaropus lobatus*), the birds of North America Online (A. Poole, Ed.) <http://bna.birds.cornell.edu/bna/species/538> (2000).
- [2] Buffon, *Histoire Naturelle des Oiseaux*, Tome 8, Imprimerie Royale, Paris (1783).
- [3] Rubega MA, Obst BS. *Auk* 1993;110:169.
- [4] Estrella SM, Masero JA, Perez-Hurtado A. *Auk* 2007;124:1244.
- [5] Rubega MA. *J Morphol* 1996;228:45.
- [6] Obst BS, et al. *Nature* 1996;384:121.
- [7] M.A. Rubega, thesis, University of California, Irvine, CA (1993).
- [8] Rubega MA. *Ibis* 1997;139:488.
- [9] Prakash M, Quéré D, Bush JWM. *Science* 2008;320:931.
- [10] Concus P, Finn R. *Phys Fluids* 1998;10:39.
- [11] Renvoisé P, Bush JWM, Prakash M, Quéré D. *EPL* 2009;86:64003.
- [12] de Gennes PG. *Colloid Polym Sci* 1986;263:463.
- [13] Bico J, Quéré D. *J Colloid Interface Sci* 2001;243:262.
- [14] Dussan V EB, Chow RTP. *J Fluid Mech* 1983;137:1.
- [15] Daniel S, Chaudhury MK. *Langmuir* 2002;18:3404.
- [16] Dong BL, Chaudhury A, Chaudhury MK. *Eur Phys J E: Soft Matter* 2006;21:231.
- [17] Shastry A, Case MJ, Böhringer KF. *Langmuir* 2006;22:6161–7.
- [18] Reyssat M, Pardo F, Quéré D. *EPL* 2009;87:36003.
- [19] Noblin X, Buguin A, Brochard-Wyart F. *Eur Phys J E* 2004;14:395.
- [20] Brunet P, Eggers J, Deegan RD. *EPJ ST* 2009;166:11.
- [21] Bush JWM, Hu D, Prakash M. *Adv Insect Physiol* 2008;34:117.